Desalination 423 (2017) 41–51

Contents lists available at ScienceDirect

Desalination

journal homepage: www.elsevier.com/locate/desal

Detailed analysis of reverse osmosis systems in hot climate conditions

S. Shaaban*, H. Yahya

Mechanical Engineering Department, College of Engineering and Technology-Cairo Campus, Arab Academy for Science, Technology and Maritime Transport (AASTMT), Cairo, Egypt

ARTICLE INFO

Keywords:
Desalination
Reverse osmosis
Membrane
Sensitivity analysis
Optimization

ABSTRACT

Hot climate countries require large amounts of desalinated water. The Reverse osmosis (RO) technique is currently considered the most reliable technique for brackish water and seawater desalination. However, its power consumption is considerably higher than all other techniques. Therefore, the present study investigates the performance of reverse osmosis plants in hot climate conditions. A typical Reverse osmosis system was designed, constructed and investigated. The ROSA software was also used for the analysis of seven different membrane elements. The experimental data were utilized in order to validate the simulation results of the ROSA software. A variance-based sensitivity analysis was performed in order to define the most effective design and operating parameters. The present investigation shows that the tap and brackish water membrane elements are more sensitive to the feed water temperature rather than the feed water pressure and concentration. Meanwhile, seawater membrane elements are more affected by the feed concentration. The detailed investigation of the different membrane elements shows that wastewater reclamation using reverse osmosis technology could be a significant source of low-cost fresh water for hot climate countries.

1. Introduction

Fresh water can be obtained in unlimited quantity by desalinating the seawater. Among the different available techniques, the Reverse Osmosis (RO) was proved to be the most reliable, cost-effective, and energy efficient in producing fresh water [1]. A major disadvantage of the reverse osmosis system is its high energy demand. Therefore, many researchers have developed simulation models for reverse osmosis systems [e.g., [2–8] in order to investigate and/or optimize their performance. The potential for developing technologies that can help in minimizing the reverse osmosis power consumption has been recently increased due to the global energy crisis and the global warming. Gelsler et al. [9] presented an energy recovery unit that implements a pressure exchange system in order to achieve considerably lower energy consumption in comparison to the conventional systems. Powering the reverse osmosis plants using renewable energy resources could significantly reduce the cost of energy. Extensive reviews of the renewable energy application in water desalination, as well as the factors influencing large-scale seawater desalination plants, were presented in Ref. [10–16]. Laborde et al. [17] presented an optimization case study for a small-scale reverse osmosis system powered by solar energy. They showed that the membrane type, area, and configuration as well as the recovery rate, and the high-pressure unit efficiency crucially affect the energy consumption. Guria et al. [18] introduced a multi-objective optimization study using the Genetic Algorithm (GA) for the desalination of seawater and brackish water using spiral wound or tubular modules. They found the membrane area to be the most important design parameter in the desalination of brackish water and seawater using spiral wound modules. Poullikkas et al. [19] developed an optimization model using a genetic algorithm for the production cost of water desalination using photovoltaics (PV). Khayet et al. [20] develop predictive models for the simulation and the optimization of reverse osmosis desalination processes. Fadaee and Radzi [21] reviewed the applied multi-objective methods that can be used for the hybrid renewable energy systems. Fraidenraich et al. [22] presented a theoretical study of the specific energy consumption of reverse osmosis devices. El-Ghonemy [23] tested a small-scale reverse osmosis system and compared his results with other available data. Vince et al. [24] developed an optimization technique for the design of reverse osmosis processes using a multi-objective optimization approach. They found that the investment cost and the operating and maintenance cost remain approximately constant for the optimal configurations. Meanwhile, the cost variations result from the influence of the operating conditions on the energy cost and the membrane replacement cost. Tzen et al. [25] presented an autonomous hybrid seawater desalination reverse osmosis system that uses the wind and solar energies. They proved that the matching of the two renewable energy resources is a feasible alternative solution for the system optimization. Bourouni et al.

* Corresponding author.
E-mail address: Sameh.Shaaban@aast.edu (S. Shaaban).

http://dx.doi.org/10.1016/j.desal.2017.09.002
Received 22 April 2017; Received in revised form 4 August 2017; Accepted 5 September 2017

List of symbols

Q_p	Permeate flux (l/m^2 hr)
R	Salt rejection (%)
SPC	Specific power consumption (kW hr./m^3)
C_f	Feed concentration (ppm)
C_p	Permeate concentration (ppm)
p	Feed pressure (bar)
T	Feed temperature (°C)
$S_T(\phi_p)_p$	Total effect index of the feed pressure on the permeate flux (−)
$S_T(Q_p)_T$	Total effect index of the feed temperature on the permeate flux (−)
$S_T(Q_p)_{CF}$	Total effect index of the feed concentration on the permeate flux (−)
$V(Q_p)\sim p$	Variance of the permeate flux at constant feed pressure (l/m^2 hr)
$V(Q_p)\sim T$	Variance of the permeate flux at constant feed temperature (l/m^2 hr)
$V(Q_p)\sim CF$	Variance of the permeate flux at constant feed concentration (l/m^2 hr)
$V(Q_p)$	Total variance of the permeate flux (l/m^2 hr)
$S_T(R)_p$	Total effect index of the feed pressure on the salt rejection (−)
$S_T(R)_T$	Total effect index of the feed temperature on the salt rejection (−)
$S_T(R)_{CF}$	Total effect index of the feed concentration on the salt rejection (−)
$V(R)\sim p$	Variance of the salt rejection at constant feed pressure (%)
$V(R)\sim T$	Variance of the salt rejection at constant feed temperature (%)
$V(R)\sim CF$	Variance of the salt rejection at constant feed concentration (%)
V(R)	Total variance of the salt rejection (%)
$S_T(SPC)_p$	Total effect index of the feed pressure on the specific power consumption (−)
$S_T(SPC)_T$	Total effect index of the feed temperature on the specific power consumption (−)
$S_T(SPC)_{CF}$	Total effect index of the feed concentration on the specific power consumption (−)
$V(SPC)\sim p$	Variance of the specific power consumption at constant feed pressure (kW hr./m^3)
$V(SPC)\sim T$	Variance of the specific power consumption at constant feed temperature (kW hr./m^3)
$V(SPC)\sim CF$	Variance of the specific power consumption at constant feed concentration (kW hr./m^3)
V(SPC)	Total variance of the specific power consumption (kW hr./m^3)

[26] presented a model based on the genetic algorithm for the coupling of a small reverse osmosis unit to different renewable energy systems. Li et al. [27] validated a previously developed optimization methodology in an industrial brackish water reverse osmosis desalination plant. They reported that a 10% reduction in the pump energy consumption was achieved when the recovery was increased from 80% to 90%. This study clearly proved the effectiveness of the model-based optimization in reverse osmosis plants operation. Sassi and Mujtaba [28] presented steady state performance predictions and optimization of the reverse osmosis process using a set of implicit mathematical equations. They achieved up to 50% reduction in the operating costs and the energy consumption using a pressure exchanger as an energy recovery device.

Water desalination using the reverse osmosis process is a multivariable complex system that requires an insight analysis of the mutual interaction between the different operating and design parameters. Hot climate countries, like Egypt and the other Arabic countries, need high quantities of desalinated water. This significantly increases the energy demand of these countries relative to the power supply and thereby affects the development of other sectors. Therefore, it is crucial to reduce the specific energy consumption of their reverse osmosis plants. The use of PV panels is not feasible for most Arabic countries due to the very high ambient temperature and the suspended dust from the desert. The wind energy is feasible for power generation at limited places. Therefore, practical solutions for the Arabic countries require an

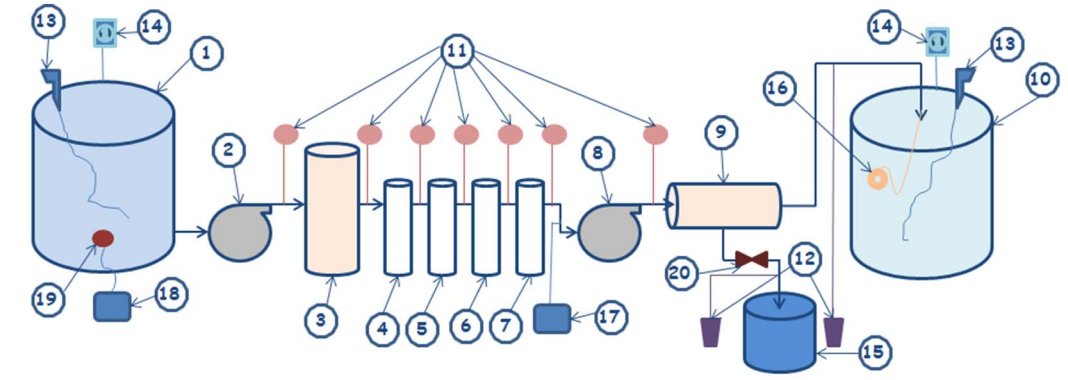

Fig. 1. Simple schematic of the experimental model.

investigation of the impact of the high feed water temperature (25–45 °C) on the performance of the reverse osmosis plants. A1-Bahri et al. [29] studied the effect of feed water temperature on the output of a MSF/SWRO hybrid plant. They reported an optimum plant output at a feed water temperature of 27–28 °C. Mohammadi et al. [30] investigated the effect of feed temperature on the membrane fouling and the permeate flux. They showed that the fouling and the permeate flux increase with the feed temperature. This behavior was also reported by Chu et al. [31]. Mohammadi et al. [30] recommended an optimum feed temperature of 35 °C for the desalination of feed water using reverse osmosis technology. Goosen et al. [32] reported 60% increase in the permeate flux when the feed temperature was increased from 20 °C to 40 °C in a spiral-wound reverse osmosis system. *Kas*i et al. [33] studied the effect of operating parameters on the membrane fouling during wastewater reclamation. Authors [e.g., [34–37]] have also proposed different designs and analysis techniques to improve the performance of reverse osmosis systems.

The above literature survey shows that the impact of the feed water temperature on the energy consumption of reverse osmosis units working in hot climate conditions was not evaluated and/or optimized. Therefore, the present work firstly investigates and analyzes the complex and mutual interaction between the feed water temperature and the other operating and design parameters for hot climate conditions (15–45 °C). Then, the specific energy consumption of reverse osmosis units was optimized for the Arabic operating conditions. Special attention was paid for reverse osmosis units in Egypt. The objective of the present work is to reduce the specific energy consumption of reverse osmosis plants by optimizing the plant location and implementing solar water heating of the feed water. Another important objective of this research is to define the most cost-effective source of desalinated water for hot climate countries (i.e., reclaiming waste water and/or desalinating seawater). In order to achieve these objectives, a detailed variance-based sensitivity analysis of seven different membranes was performed. The feed water temperature was considered within the typical operating conditions of hot climate countries. The ROSA software was utilized to simulate the performance of the selected membranes under different operating conditions. One of the selected membranes was experimentally tested in order to validate the theoretical model of the ROSA software before implementing it in an extensive theoretical investigation of different membrane elements under varying operating conditions.

2. Test rig design and construction

A reverse osmosis experimental model was established and the effect of the different design and operating parameters on its power consumption was experimentally investigated. A simple schematic of the experimental model is shown in Fig. 1.

The system implements a pump (part no. 2) that feeds the saline water from a feed tank (part no. 1) to the pretreatment stages. A typical saline feed water contains various concentrations of dissolved matter and suspended solids. Therefore, five successive stages were used in order to prevent membrane contamination, fouling, scaling, and degradation. The first stage is a multimedia filter (part no. 3) that removes the suspended particles from the feed water. The second stage contains a five-micron cartridge filter (part no. 4) that prevents the membrane fouling by suspended particles larger than five microns in diameter. The third stage is an activated carbon cartridge filter (part no. 5) that removes the dissolved organic materials and chlorine compounds. The fourth stage comprises a softener resin cartridge filter (part no. 6) to minimize precipitation and scaling. The last stage contains a one-micron cartridge filter (part no. 7) to retain suspended particles that are larger than one micron in diameter. A high-pressure pump (part no. 8) was used in order to overcome the osmotic pressure of the salt solution and force the water through the semipermeable membrane. The membrane retains the dissolved salts and the organic molecules.

Various samples of feed water with a feed concentration ranging from 100 to 2000 ppm were experimentally tested in the present study. A single stage centrifugal pump operating at a constant pressure of about 2.6 bar (part no. 2) was used to feed saline water to the pretreatment stages. Another single stage centrifugal pump (part no. 8) was used as a high-pressure pump operating from 0.6 to 4 bar head and 0.16 to 0.35 m^3/h flow rate. A FILMTEC™ TW30-4040 housed in a stainless steel pressure vessel (part no. 9) was used to remove dissolved salts from the feed water. An electrical heater of 12 V/600 W (part no. 19) was connected to the insulated feed water tank and a digital temperature controller (part no. 18) was utilized to change and/or control the feed water temperature.

Measurements of the feed water salt concentration, pressure, flow rate, and temperature as well as the permeate water salt concentration and flow rate should be carried out accurately. Therefore, pressure gauges, thermocouples, flowmeters, and conductivity meters were calibrated and connected to the system in order to study the operating and the performance parameters of the system. Pressure gauges (part no. 11) ranging from 0 to 10 bar with an accuracy of ± 0.1 bar were used to measure the pressure drop across the pretreatment stages as well as the discharge pressure of the feed pump and the high-pressure pump. Two identical rotameters (part no. 12) ranging from 0 to 18 l/min with an accuracy of ± 0.4 l/min were used to measure the permeate water flow rate and the concentrate water flow rate. A K-type thermocouple (part no. 13) with an accuracy of ± 0.2 °C was utilized to measure the feed water temperature. Conductivity meters (part no. 14) with an accuracy of ± 1 μS/cm were used to monitor the water conductivity in order to evaluate the feed water salt concentration and the permeate water salt concentration. One conductivity meter was inserted in the feed water tank and another one was placed inside the product tank (part no. 10). Consequently, the salt rejection rate (R) was estimated from

$$R = \frac{C_f - C_p}{C_f} \times 100 \quad (1)$$

where C_f and C_p are the feed concentration and permeate concentration, respectively.

3. Experimental results

The present work evaluates the performance of the reverse osmosis plants in hot climate conditions with a special focus on the specific energy consumption. Therefore, a FILMTEC™ TW30-4040 membrane was experimentally tested under different values of the feed water concentration, pressure, and temperature. The performance of the reverse osmosis system is expressed in terms of the permeate flux, salt rejection, and specific power consumption. The membrane permeate flux describes the produced volume flow rate per unit area of the membrane. The salt rejection represents the percentage salt removed from the feed water, while the specific power consumption can be defined as the power consumed by a reverse osmosis system to produce a specific volume flow rate of water.

Feed water with salt concentration ranging from 100 ppm to 2000 ppm was supplied at a feed pressure that varies from 2.6 bar to 6 bar and water temperature between 15 °C to 35 °C. The pump feed rate varies from 0.35 m^3/h at 2.6 bar to 0.16 m^3/h at 6 bar. The system performance parameters were accurately measured under these operating conditions. For validation purposes, the same experimental model was simulated using the software ROSA under the same operating conditions. Comparisons between the measured and the simulated performance are presented in Figs. 2–10. Fig. 2 shows very good agreement between the measured and the simulated performance. The permeate flux across the membrane is directly proportional to the feed water pressure at constant feed temperature (35 °C). Meanwhile, higher salt concentrations at constant feed temperature (35 °C) results in lower

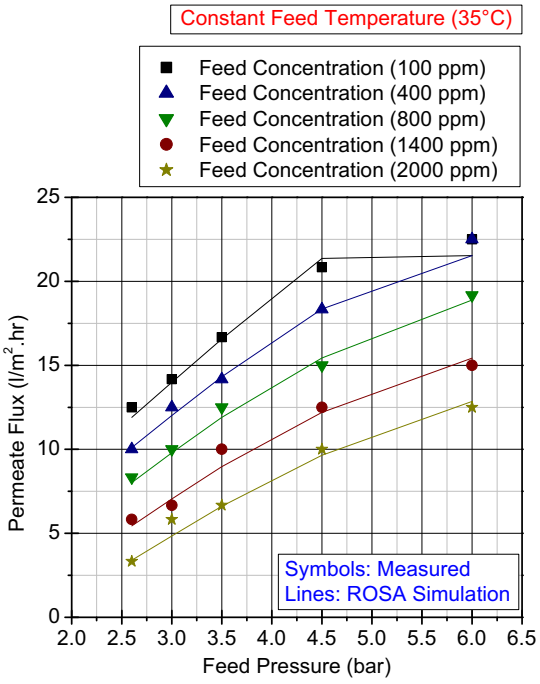

Fig. 2. Effect of pressure and feed concentration on permeate flux at constant feed temperature.

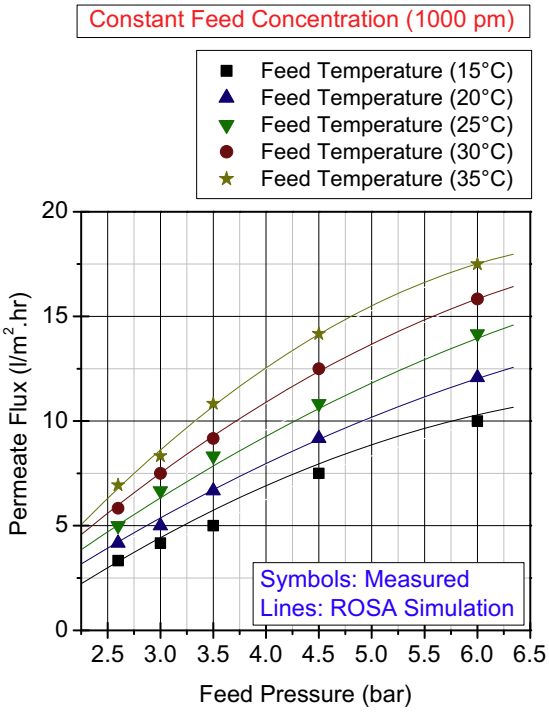

Fig. 3. Effect of pressure and temperature on permeate flux at constant feed concentration.

permeate flux. This is because the reverse osmosis units apply pressure to the feed water stream to overcome the natural osmotic pressure. The osmotic pressure increases with increasing the salt concentration of the feed water. Therefore, increasing the feed pressure and reducing the feed concentration increase the permeate flux. The membrane has a 100% recovery at feed pressure 6 bar, feed temperature 35 °C, and concentration ≤ 400 ppm. Therefore, the permeate flux at 100 ppm equals that at 400 ppm for a feed pressure and temperature of 6 bar and 35 °C, respectively.

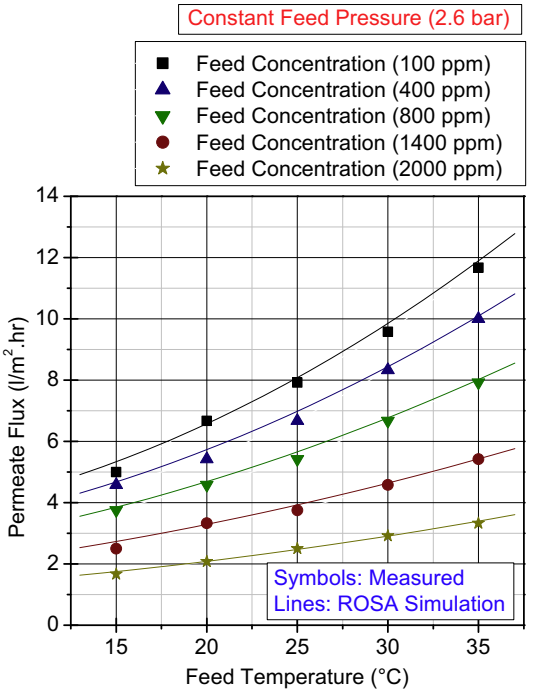

Fig. 4. Effect of feed temperature and concentration on permeate flux at constant feed pressure.

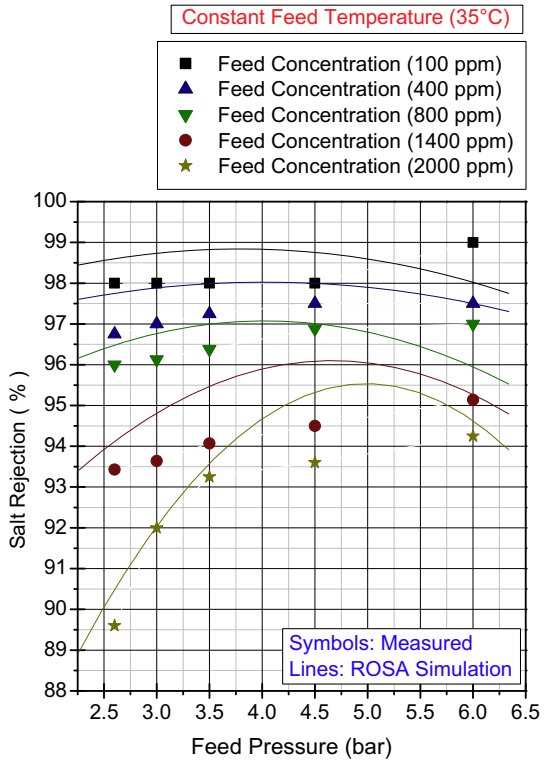

Fig. 5. Effect of pressure and feed concentration on salt rejection at constant feed temperature.

Fig. 3 shows that the permeate flux is directly dependent on the feed water temperature at a constant feed concentration of 1000 ppm. The membrane productivity was found to be highly dependent on changes in the feed water temperature. The permeate flux increases with increasing the feed water temperature due to the changes in the physical properties of the polymeric membrane such as the pore size. This results

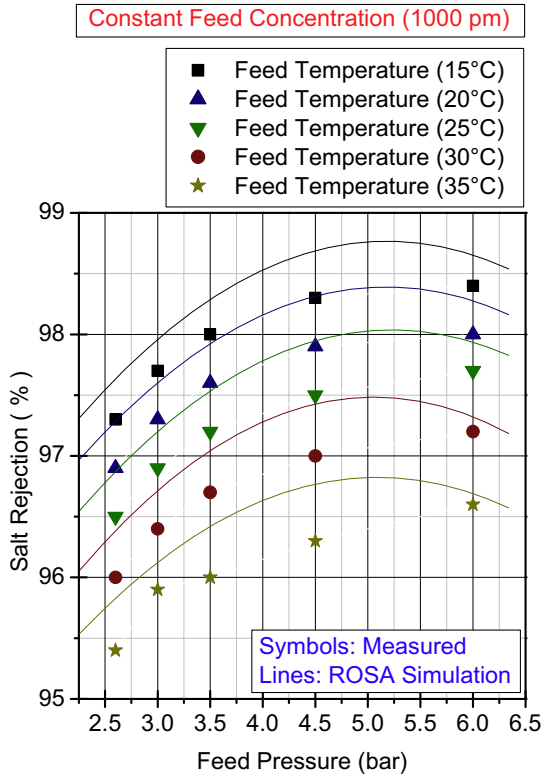

Fig. 6. Effect of pressure and temperature on salt rejection at constant feed concentration.

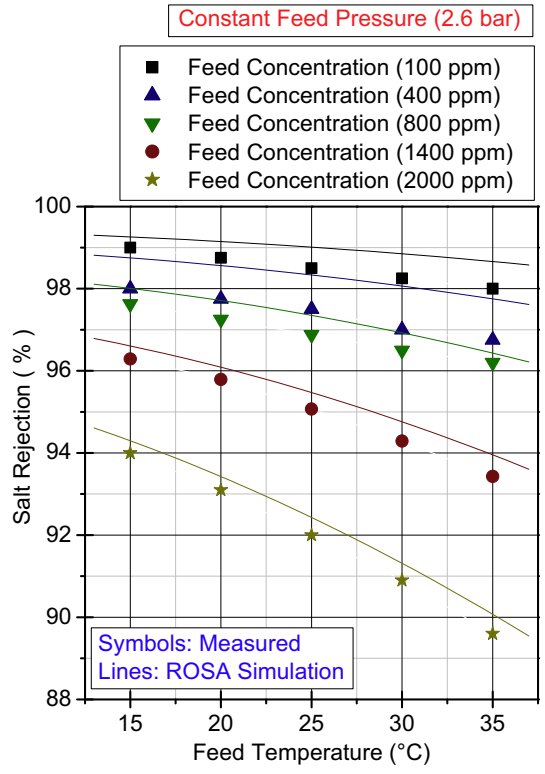

Fig. 7. Effect of temperature and feed concentration on permeate flux at constant feed pressure.

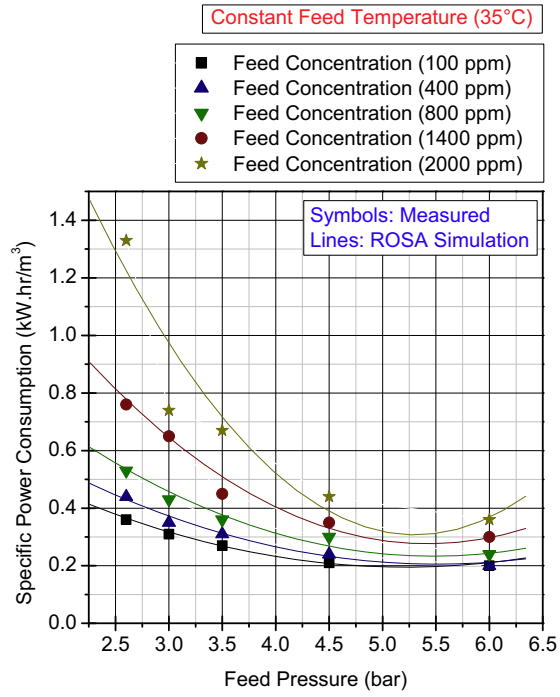

Fig. 8. Effect of pressure and feed concentration on permeate power consumption at constant feed temperature.

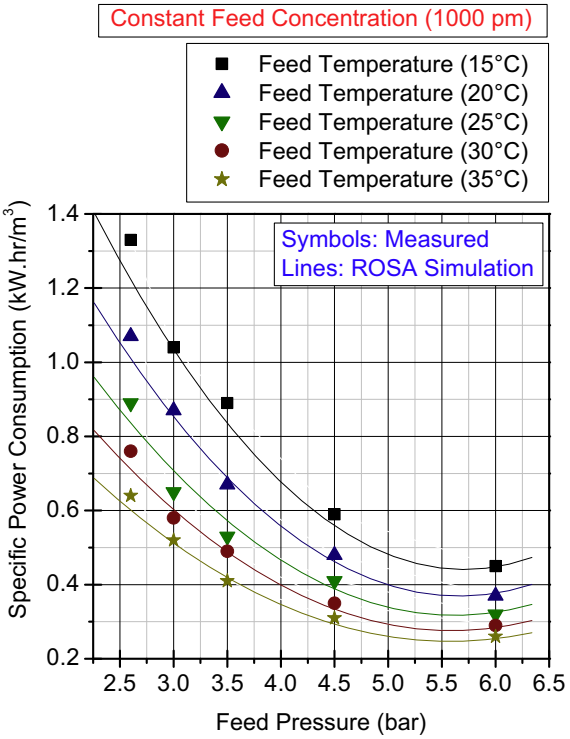

Fig. 9. Effect of pressure and temperature on permeate power consumption at constant feed concentration.

in higher water diffusion rate through the membrane. Meanwhile, increasing the feed water concentration at constant feed pressure reduces the permeate flux as shown in Fig. 4. The permeate flux increases with increasing the feed water pressure due to the expansion of the salt passages. Consequently, the feed water is pushed through the membrane at a higher rate. The increased feed water pressure also increases the salt rejection as shown in Figs. 5 and 6. In contrast, the increased feed water concentration at constant feed water temperature (35 °C) results in lower salt rejection as shown in Fig. 5. Increasing the feed water temperature at constant feed water concentration (1000 ppm) also results in lower salt rejection as shown in Fig. 6. This is due to the

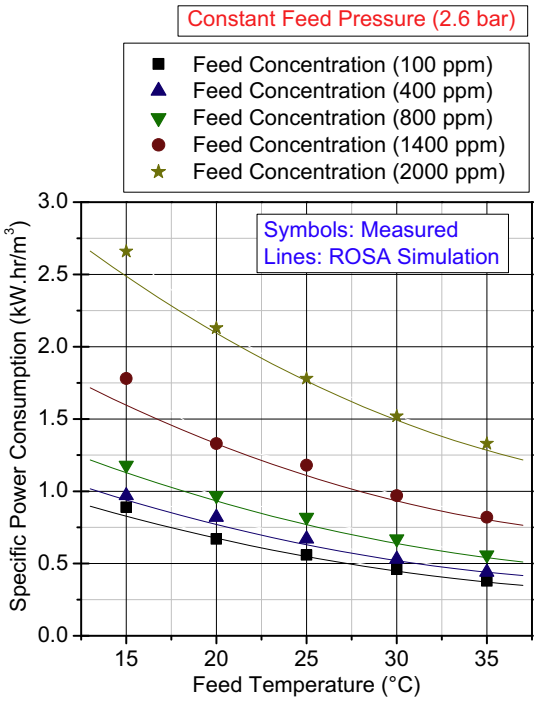

Fig. 10. Effect of temperature and feed concentration on power consumption at constant feed pressure.

higher salt diffusion rate through the membrane at higher feed water temperatures. For the same feed water pressure (2.6 bar), increasing the feed water concentration reduces the membrane salt rejection as shown in Fig. 7.

The specific power consumption is the key parameter of the present investigation. Fig. 8 shows that the specific power consumption decreases with increasing the feed water pressure at constant feed temperature (35 °C). This is due to the increase in the permeate flux with increasing the feed water pressure as shown in Fig. 3.

Figs. 9 and 10 show that the specific power consumption decreases with increasing the feed water temperature at constant feed water concentration (1000 ppm) but increases with increasing the feed water concentration. This is because increasing the feed water temperature improves the permeate flux across the membrane as shown in Fig. 4. Therefore, the specific power consumption decreases as a result of increasing the permeate flux. This means that the cost of water desalination using reverse osmosis plants will be better for hot climate countries due to the higher temperature of the feed water. Fig. 10 shows that, for the same feed water pressure (2.6 bar), increasing the feed water concentration increases the specific power consumption due to the reduction of the permeate flux across the membrane, Fig. 2.

The experimental results show good agreement with the simulation results of the ROSA software. Therefore, the simulation model was validated and other types of membranes will be simulated using the ROSA software rather than being experimentally investigated.

4. Variance based sensitivity analysis

The experimental results highlighted a significant dependence of the specific power consumption of reverse osmosis units on the feed water temperature. This effect is mutually interacting with other operating parameters like the feed water pressure and salt concentration. Moreover, the membrane type could also be a significant parameter. Therefore, a variance-based sensitivity analysis was carried out in order to obtain a clear vision of the design and operating parameters that significantly affect the specific power consumption of reverse osmosis units in hot climate conditions. Consequently, the temperature was considered with much care in the present investigation.

A system output parameter (Y) (i.e., Permeate flux Q_p, salt rejection R, and specific power consumption (SPC)) can be considered as a function of the input parameters (i.e., feed concentration C_f, pressure p, and temperature T). These functions can be written as follows [38,39]

$$Q_p = f(C_f, p, T) \tag{2}$$

$$R = f(C_f, p, T) \tag{3}$$

$$SPC = f(C_f, p, T) \tag{4}$$

The total variance of a system output V(Y) can be defined as the summation of the partial variances of the individual input parameters $\Sigma_i^n V_i$ and the partial variances for the interaction of two input parameters $\Sigma_i^n \Sigma_{j>i}^n V_{ij}$

$$V(Y) = \sum_i^n V_i + \sum_i^n \sum_{j>i}^n V_{ij} \tag{5}$$

The dimensionless first-order sensitivity index of each input on the system output is defined as follows [12]

$$S_i = \frac{V_i}{V(Y)} \tag{6}$$

The input parameters (i.e., feed concentration C_f, pressure p, and temperature T) are considered independent of each other. Therefore, the dimensionless total effect index for each independent parameter can be obtained from the following equations:

$$S_T(Q_p)_p = 1 - \frac{V(Q_p)\sim p}{V(Q_p)} \tag{7}$$

$$S_T(Q_p)_T = 1 - \frac{V(Q_p)\sim T}{V(Q_p)} \tag{8}$$

$$S_T(Q_p)_{CF} = 1 - \frac{V(Q_p)\sim CF}{V(Q_p)} \tag{9}$$

where $S_T(\phi_p)_P$ is the total effect index of the feed pressure on the permeate flux, $S_T(Q_p)_T$ is the total effect index of the feed temperature on the permeate flux, $S_T(Q_p)_{CF}$ is the total effect index of the feed concentration on the permeate flux, $V(Q_p)\sim p$ is the variance of the permeate flux at constant feed pressure, $V(Q_p)\sim T$ is the variance of the permeate flux at constant feed temperature, $V(Q_p)\sim CF$ is the variance of the permeate flux at constant feed concentration and $V(Q_p)$ is the total variance of the permeate flux.

Similarly, the following equations demonstrate the total effect index S_{Ti} for the feed pressure, temperature, and concentration on the salt rejection:

$$S_T(R)_p = 1 - \frac{V(R)\sim p}{V(R)} \tag{10}$$

$$S_T(R)_T = 1 - \frac{V(R)\sim T}{V(R)} \tag{11}$$

$$S_T(R)_{CF} = 1 - \frac{V(SR)\sim CF}{V(R)} \tag{12}$$

where $S_T(R)_P$ is the total effect index of the feed pressure on the salt rejection, $S_T(R)_T$ is the total effect index of the feed temperature on the salt rejection, $S_T(R)_{CF}$ is the total effect index of the feed concentration on the salt rejection, $V(R)\sim P$ is the variance of the salt rejection at constant feed pressure, $V(R)\sim T$ is the variance of the salt rejection at constant feed temperature, $V(SR)\sim CF$ is the variance of the salt rejection at constant feed concentration and V(R) is the total variance of the salt rejection.

The total effect index S_{Ti} of the feed pressure, temperature and concentration on the specific power consumption can also be presented as follows

$$S_T(SPC)_P = 1 - \frac{V(SPC)\sim P}{V(SPC)} \quad (13)$$

$$S_T(SPC)_T = 1 - \frac{V(SPC)\sim T}{V(SPC)} \quad (14)$$

$$S_T(SPC)_{CF} = 1 - \frac{V(SPC)\sim CF}{V(SPC)} \quad (15)$$

where $S_T(SPC)_P$ is the total effect index of the feed pressure on the specific power consumption, $S_T(SPC)_T$ is the total effect index of the feed temperature on the specific power consumption, $S_T(SPC)_{CF}$ is the total effect index of the feed concentration on the specific power consumption, $V(SPC)\sim P$ is the variance of the specific power consumption at constant feed pressure, $V(SPC)\sim T$ is the variance of the specific power consumption at constant feed temperature, $V(SPC)\sim CF$ is the variance of the specific power consumption at constant feed concentration and V(SPC) is the total variance of the specific power consumption.

The variance-based sensitivity analysis was performed for seven different samples of membranes. Table 1 summarizes the main performance attributes of the investigated membrane elements. The validated ROSA simulation model was used in order to estimate the performance of these membrane elements under different operating conditions. Figs. 11–13 introduce the total effect index of the feed pressure on the permeate flux, salt rejection, and specific power consumption. Figs. 14–16 show the total effect index of the feed temperature on the performance parameters, while the total effect index of the feed concentration on the performance parameters is shown in Figs. 17–19.

Fig. 11 shows that the total effect index of the feed pressure on the permeate flux $S_T(\phi_p)_P$for the tap and brackish water membrane elements is greater than that of the seawater membrane elements. The total effect index of the feed pressure on the salt rejection $S_T(R)_P$ for the tap and brackish water membrane elements is also greater than that of the seawater membrane elements as shown in Fig. 12. Fig. 13 demonstrates that the total effect index of the feed pressure on the specific power consumption $S_T(SPC)_P$ for brackish water membrane elements is greater than that of the tap and the seawater membrane elements. The specific power consumption of the tap water membrane element is slightly less sensitive to the feed pressure compared to the seawater membrane elements. The extra low energy membrane has the lowest sensitivity to the feed pressure.

Fig. 14 shows that the total effect index of the feed temperature on the permeate flux $S_T(\phi_p)_T$for the tap and brackish water membrane elements is greater than that of the seawater membrane elements. Meanwhile, the total effect index of the feed temperature on the salt rejection $S_T(R)_T$ is convergent for the various types of membrane elements, Fig. 15. The specific power consumption of the tap and brackish water membrane elements is much sensitive to the feed temperature compared to the seawater membrane elements as shown in Fig. 16. This highlights the feasibility of wastewater reclamation at low cost for hot climate countries using the reverse osmosis technology.

Figs. 17–19 show that the total effect index of the feed concentration on the permeate flux $S_T(\phi_p)_{CF}$, the salt rejection $S_T(R)_{CF}$, and the specific power consumption $S_T(SPC)_{CF}$ for the seawater membrane elements is greater than those of the tap and brackish water membrane elements. Therefore, the specific power consumption of wastewater reclaiming in hot climate conditions will be much lower than that of desalinating the seawater.

The above analysis shows that all operating conditions significantly affect the performance of reverse osmosis plants. The specific power consumption of tap and brackish water membrane elements is more affected by the feed water temperature and less affected by the feed concentration. Therefore, wastewater reclamation can be an important source of fresh water for hot climate conditions. The feed temperature has also a tangible influence on the specific power consumption of seawater membrane elements. In order to evaluate this effect, reverse osmosis plants were designed to handle sea water at concentrations of 37,800 ppm, 42,000 ppm, and 50,000 ppm. The 37,800 ppm concentration represents an average salinity of the Mediterranean Sea near Egypt [40,41] while the 42,000 ppm corresponds to the red sea average salinity [42]. The 50,000 ppm salinity could be found in the gulf water near Saudi Arabia, Kuwait, and the United Arab Emirates [43]. The three reverse osmosis plants were designed using the ROSA software to provide a 50% recovery at an operating temperature of 28 °C. The design feed water temperature was selected close to the recommended optimum value [29]. The membrane elements SW30XLE-400i and SW30HR-380 were implemented to provide high salt rejection and productivity (Table 1). The membrane element SW30XLE-400i is a low energy element while the SW30HR-380 is a high energy element. All performance parameters of the three plants were normalized using the design data at feed concentration 38,700 ppm (design temperature T_{des} = 28 °C and design recovery R_{des} = 50%). Fig. 20 presents the normalized specific energy at different feed concentrations and temperatures. The normalized temperature is the ratio between the feed temperature and the design feed temperature (T_{des} = 28 °C). The normalized specific energy represents the ratio between the specific energy consumption and the specific energy consumption for salt concentration 38,700 ppm, 50% recovery, and feed temperature T_{des} = 28 °C. Fig. 20 shows 1–3% reduction of the specific energy consumption using the low energy SW30XLE-400i membrane element at a moderate salt concentration of 42,000 ppm. Both membrane elements consume almost the same specific energy at salt concentration 38,700 ppm and 50,000 ppm. The low energy membrane element is recommended for the red sea (salt concentration 38,700 ppm) while both elements can be used at the northern coast of Egypt. These results clearly show that each sea location may have different optimum membrane element.

The specific energy consumption of the low energy and the high energy membrane elements significantly increases with salt concentration as shown in Fig. 20. Moreover, about 12.8% reduction of the specific energy takes place by increasing the feed water temperature from 15 °C to 45 °C. Accordingly, increasing the feed water temperature is favorable from energy point of view. However, it increases the membrane fouling, cleaning cycles, and the scaling problems. Therefore, an economical optimization of the feed water temperature is recommended for future work to solve the tradeoff between the low specific energy consumption and the long membrane life time and water quality. This is because the salt rejection tangibly decreases at high values of the feed water temperature as shown in Fig. 21. The reduction of the salt rejection with feed water temperature is higher at salt concentration 50,000 ppm.

Fig. 22 shows that the membrane recovery significantly increases with increasing the feed water temperature. Accordingly, all plant performance parameters are highly dependent on the feed water temperature. About 14% increase of the recovery could be achieved by heating the feed water from 15 °C to 45 °C.

The above analysis highlights the significant dependence of the reverse osmosis plant performance on the feed water temperature. For

Table 1
Specifications of the investigated membrane elements.

Element	Water type	Performance attributes
XLE-440	Brackish	Low Energy - Low Salt Rejection -High Productivity
BW30-400	Brackish	High Energy - High Productivity
TW30-4040	Tap	High Energy - Low Productivity
SW30-4040	Sea	High Energy - Low Salt Rejection -Low Productivity
SW30HR-380	Sea	High Energy - High Salt Rejection
SW30HRLE-400i	Sea	Low Energy - High Salt Rejection
SW30XLE-400i	Sea	Low Energy - High Salt Rejection -High Productivity

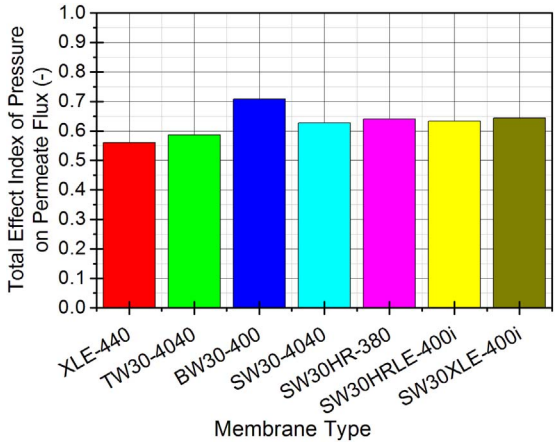

Fig. 11. Total effect index of the feed pressure on the permeate flux.

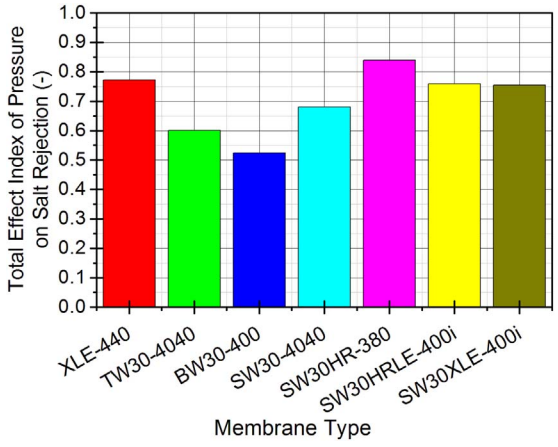

Fig. 12. Total effect index of the feed pressure on the salt rejection.

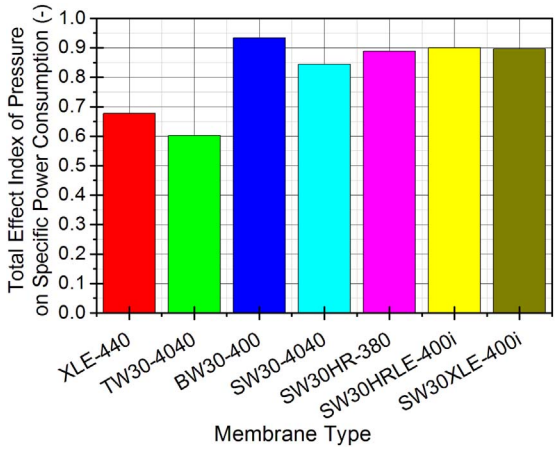

Fig. 13. Total effect index of the feed pressure on the specific power consumption.

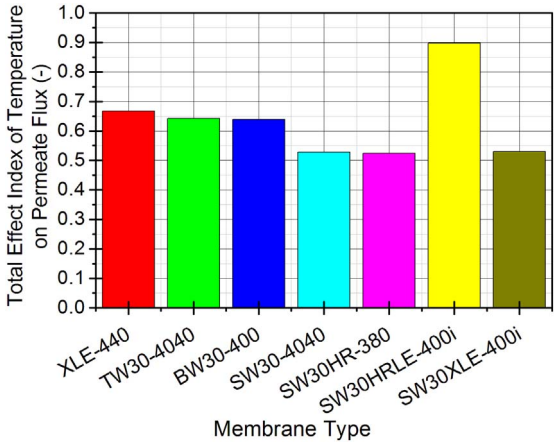

Fig. 14. Total effect index of the temperature on the permeate flux.

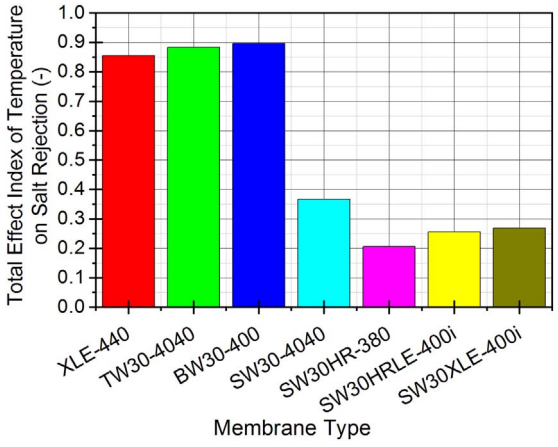

Fig. 15. Total effect index of the temperature on the salt rejection.

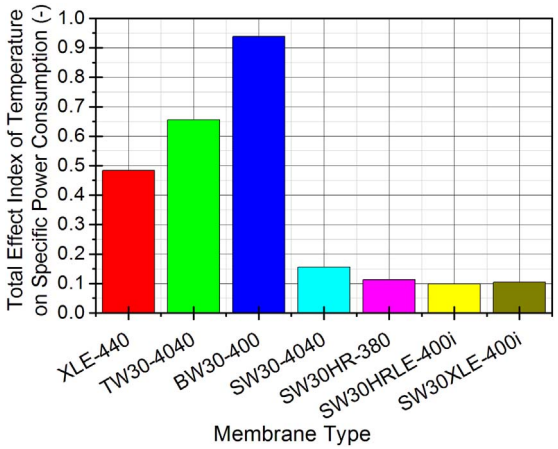

Fig. 16. Total effect index of the temperature on the specific power consumption.

hot climate countries, the selection of the reverse osmosis plant location must consider both the salinity and the feed water temperature. Reverse osmosis desalination units are found in Egypt at the red sea (e.g. Hurghada and Sharm El-Sheikh) and the Mediterranean Sea (e.g., Matrouh). The monthly averaged sea water temperature at Hurghada, Sharm El-Sheikh, and Matrouh was obtained from the World Sea Temperature. The average salinity at Hurghada, Sharm El-Sheikh is 42,000 ppm [42] while that at Matrouh is 38,700 ppm [40,41]. Both the low energy SW30XLE-400i and the high energy SW30HR-380 membrane elements were simulated at the three locations for the twelve months of the year. The results show that both Hurghada and Sharm El-Sheikh have almost the same annual specific power consumption with Sharm El-Sheikh slightly lower than Hurghada. This is because both have the same average salinity but the sea temperature at Sharm El-Sheikh is slightly higher than that at Hurghada.

Figs. 23 and 24 show the monthly average specific energy consumption of the low energy SW30XLE-400i and the high energy SW30HR-380 membrane elements. The highest sea water temperatures take place in August where the feed water reaches an average temperature of 28.8 °C in Sharm El-Sheikh and 27.4 °C in Matrouh. Both

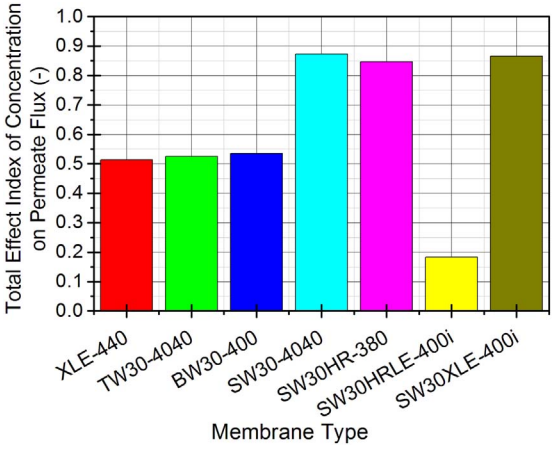

Fig. 17. Total effect index of the feed concentration on the permeate flux.

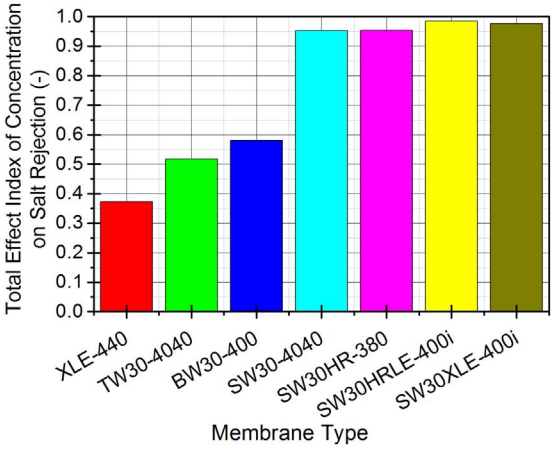

Fig. 18. Total effect index of the feed concentration on the salt rejection.

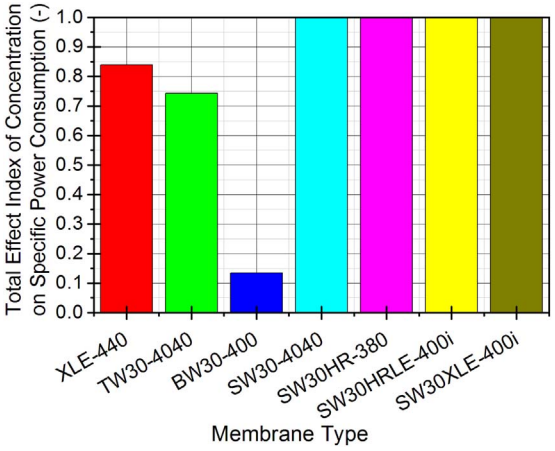

Fig. 19. Total effect index of the feed concentration on the specific power consumption.

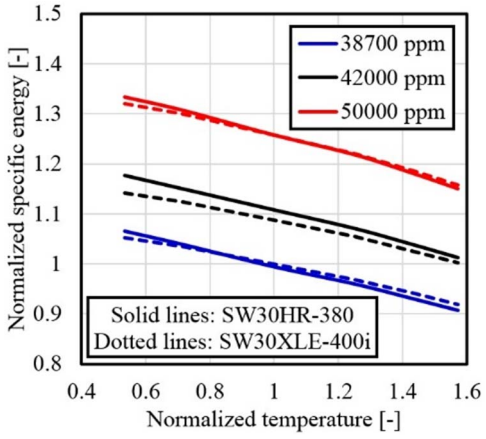

Fig. 20. Variation of the specific energy with feed temperature and concentration.

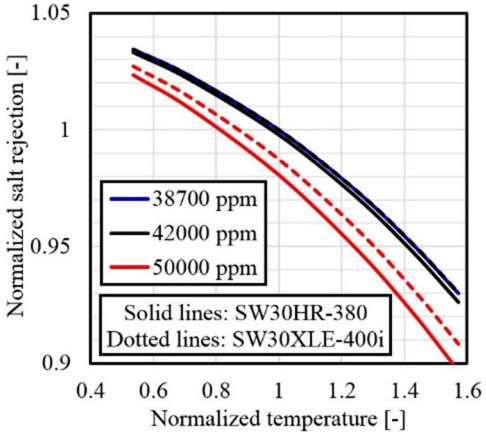

Fig. 21. Variation of the salt rejection with feed temperature and concentration.

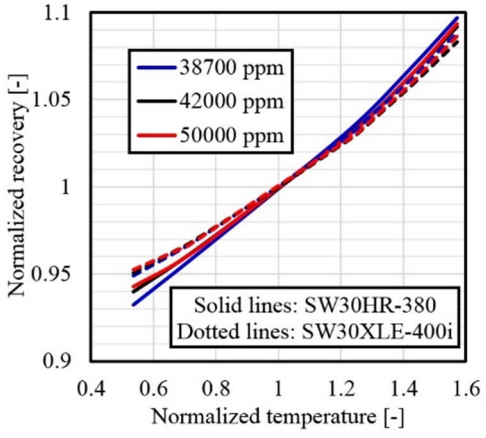

Fig. 22. Variation of the membrane recovery with feed temperature and concentration.

conditions are very close to the optimum feed temperature suggested by Al-Bahri et al. [29] for MSF/SWRO hybrid plant. Therefore, this type of plants is very promising for use in Egypt. The low energy membrane element consumes tangibly lower specific energy for plants operating at Hurghada and Sharm El-Sheikh. Meanwhile, the high and low membrane elements consume comparable energy at Matrouh. Reverse osmosis plants at Matrouh consumes about 5.5–7.8% less energy compared to those at Hurghada and Sharm El-Sheikh due to the lower sea salinity. The sea water temperature at Matrouh is tangibly lower than that at Hurghada and Sharm El-Sheikh in winter months. Therefore, solar water heating can be implemented in order to maintain the feed water at the optimum temperature all over the year. With solar heating to an optimum feed water temperature of 35 °C as recommended by Mohammadi et al. [30], the specific energy consumption at Matrouh (as well as the entire northern coast of Egypt) could be reduced by up to 9.5% during winter months and 6.7% for the entire year. Meanwhile, solar feed water heating to 35 °C reduces the specific energy consumption at Hurghada and Sharm El-Sheikh by an annual average of 4.5%. A reverse osmosis plant with solar feed water heating in the northern sea of Egypt will consume 8.4% less energy compared to the same plant at Hurghada and Sharm El-Sheikh. Therefore, Egypt has the

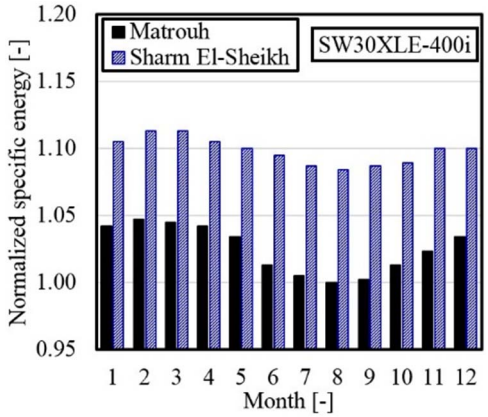

Fig. 23. Annual specific energy consumption of the low energy membrane at Matrouh and Sharm El-Sheikh.

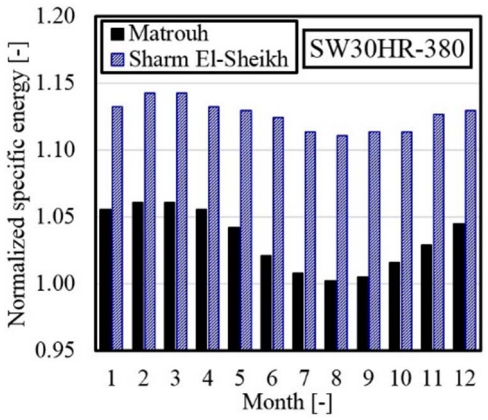

Fig. 24. Annual specific energy consumption of the high energy membrane at Matrouh and Sharm El-Sheikh.

potential to produce desalinated water at considerably lower specific energy by hybridizing the solar heating with the reverse osmosis plants.

The present study showed clearly that there is a high potential for reducing the specific power consumption of reverse osmosis plants operating in hot climate conditions. The specific power consumption of the tap and brackish membrane elements is more sensitive to the feed water temperature. Therefore, wastewater reclamation could present a cost-effective solution for hot climate countries.

5. Conclusion

The present study thoroughly investigated the effect of the different operating parameters on the performance of reverse osmosis systems with different membrane elements. It focuses on the specific power consumption of the different membrane elements. Special attention was paid to the effect of the feed water temperature. This is because hot climate countries need more desalinated water compared to other countries. A variance-based sensitivity analysis was implemented for seven different samples of membranes. The investigated membrane elements are suitable for tap, brackish, and seawater. The following conclusions can be drawn:

a. The permeate flux of the tap and brackish water membrane elements is more sensitive to the feed pressure. However, the feed temperature affects the permeate flux of the tap and brackish water membrane elements more than the feed concentration.
b. The permeate flux of the seawater membrane elements is more sensitive to the feed concentration. The seawater membrane elements have also higher total effect index of the feed pressure on the permeate flux compared to the total effect index of the feed temperature. However, the effect of the feed temperature is tangible and cannot be ignored.
c. The feed temperature has a significant effect on the salt rejection of all membrane types. The temperature effect is convergent for the tap, brackish, and seawater membrane elements.
d. The salt rejection of the tap and brackish water membrane elements is more affected by the feed temperature, then the feed pressure, and finally the feed concentration. Meanwhile, the salt rejection of the seawater membrane elements is more affected by the feed temperature, then the feed concentration, and finally the feed pressure.
e. The specific power consumption of the tap and brackish water membrane elements is significantly sensitive to the feed water temperature. The feed pressure and concentration have convergent effects on the specific power consumption of the tap and brackish water membrane elements. Therefore, the present study highlights the wastewater reclamation using reverse osmosis technique as an important source of fresh water in hot climate conditions from both the permeate flux and the specific power consumption points of view.
f. The specific power consumption of the seawater membrane elements is more dependent on the feed concentration compared to the feed pressure. It also clearly depends on the feed temperature. Therefore, reverse osmosis plants operating in hot climate conditions can perform better than those operating in low-temperature conditions.
g. In general, wastewater reclamation could be a more cost-effective solution for hot climate countries compared to the seawater desalination. A full economic study of the wastewater reclamation in hot climate conditions is recommended for future work.

Appendix A. Supplementary data

Supplementary data to this article can be found online at http://dx.doi.org/10.1016/j.desal.2017.09.002.

References

[1] A. Al-Karaghouli, K. Larry, Economic and technical analysis of a reverse-osmosis water desalination plant using DEEP-3.2 software, J. Environ. Sci. Eng. 1 (3A) (2012) 318.
[2] E. Tzen, K. Perrakis, P. Baltas, Design of a standalone PV desalination system for rural areas, Desalination 119 (1998) 327–333.
[3] K. Jamala, M.A. Khan, M. Kamil, Mathematical modeling of reverse osmosis systems, Desalination (1) (2004) 29–42.
[4] Z. Al Suleimani, V.R. Nair, Desalination by solar-powered reverse osmosis in a remote area of the Sultanate of Oman, Appl. Energy 65 (2000) 367–380.
[5] M. Thomson, D. Infield, A photovoltaic-powered seawater reverse-osmosis system without batteries, Desalination 153 (2002) 1–8.
[6] E.S. Mohamed, G. Papadakis, Design, simulation and economic analysis of a standalone reverse osmosis desalination unit powered by wind turbines and photovoltaics, Desalination 164 (2004) 87–97.
[7] M. Li, Optimal plant operation of brackish water reverse osmosis (BWRO) desalination, Desalination 293 (2012) 61–68.
[8] R. Pohl, M. Kaltschmitta, R. Holländerb, Investigation of different operational strategies for the variable operation of a simple reverse osmosis unit, Desalination 249 (3) (2009) 1280–1287.
[9] P. Gelsler, W. Krumm, T. Peters, Optimization of the energy demand of reverse osmosis with a pressure-exchange system, Desalination 125 (1999) 167–172.
[10] E. Mathioulaks, V. Belessiotis, E. Delyannis, Desalination by using alternative energy: review and state-of-the-art, Desalination 203 (2007) 346–365.
[11] M.A. Eltawil, Z. Zhengming, L. Yuan, A review of renewable energy technologies integrated with desalination systems, Renew. Sust. Energ. Rev. 13 (2009) 2245–2262.
[12] K. Bourouni, T. Ben M'Barek, A. Al Taee, Design and optimization of desalination reverse osmosis plants driven by renewable energies using genetic algorithms, Renew. Energy 36 (2011) 936–950.
[13] A.M.K. El-Ghonemy, Water desalination systems powered by renewable energy sources: review, Renew. Sust. Energ. Rev. 16 (2012) 1537–1556.
[14] M. Shatat, M. Worall, S. Riffat, Opportunities for solar water desalination worldwide: review, Sustainable Cities and Society, 9 2013, pp. 67–80.
[15] C. Li, Y. Goswami, E. Stefanakos, Solar assisted sea water desalination: a review, Renew. Sust. Energ. Rev. 19 (2013) 136–163.
[16] Y.M. Kim, S.J. Kim, Y.S. Kim, S. Lee, I.S. Kim, J.H. Kim, Overview of systems

engineering approaches for a large-scale seawater desalination plant with a reverse osmosis network, Desalination 238 (2009) 312–332.
[17] H.M. Laborde, K.B. França, H. Neff, A.M.N. Lima, Optimization strategy for a small-scale reverse osmosis water desalination system based on solar energy, Desalination 133 (2001) 1–12.
[18] C. Guria, P.K. Bhattachary, S.K. Gupta, Multi-objective optimization of reverse osmosis desalination units using different adaptations of the non-dominated sorting genetic algorithm (NSGA), Comput. Chem. Eng. 29 (2005) 1977–1995.
[19] A. Poullikkas, An optimization model for the production of desalinated water using photovoltaic systems, Desalination 258 (2010) 100–105.
[20] M. Khayet, M. Essalhi, C. Armenta-Déu, C. Cojocaru, N. Hilal, Optimization of solar-powered reverse osmosis desalination pilot plant using response surface methodology, Desalination 261 (2011) 284–292.
[21] M. Fadaee, M.A.M. Radzi, Multi-objective optimization of a stand-alone hybrid renewable energy system by using evolutionary algorithms: a review, Renew. Sust. Energ. Rev. 16 (5) (2012) 3364–3369.
[22] N. Fraidenraich, O.C. Vilela, G.A. Lima, Specific energy consumption of PV reverse osmosis systems. Experiment and theory, Prog. Photovolt. (2012), http://dx.doi.org/10.1002/pip.1239.
[23] A.M.K. El-Ghonemy, RETRACTED: a small-scale brackish water reverse-osmosis desalination system used in northern Saudi Arabia: a case study, Renew. Sust. Energ. Rev. 16 (7) (2012) 4597–4605.
[24] F. Vince, F. Marechal, E. Aoustin, P. Bréant, Multi-objective optimization of RO desalination plants, Desalination 222 (2008) 96–118.
[25] E. Tzen, D. Theofilloyianakos, Z. Kologios, Autonomous reverse osmosis units driven by RE sources experiences and lessons learned, Desalination 221 (2008) 29–36.
[26] K. Bourouni, T. Ben M'Barek, A. Al Taee, Design and optimization of desalination reverse osmosis plants driven by renewable energies using genetic algorithms, Renew. Energy 36 (2011) 936–950.
[27] M. Li, B. Noh, Validation of model-based optimization of brackish water reverse osmosis (BWRO) plant operation, Desalination 304 (2012) 20–24.
[28] K.M. Sassi, I.M. Mujtaba, Simulation and optimization of full scale reverse osmosis desalination plant, Comput. Chem. Eng. 59 (2013) 101–110.
[29] Z.K. Al-Bahri, W.T. Hanbury, T. Hodgkiess, Optimum feed temperatures for seawater reverse osmosis plant operation in an MSF/SWRO hybrid plant, Desalination 138 (2001) 335–339.
[30] T. Mohammadi, M.K. Moghadam, S.S. Madaeni, Hydrodynamic factors affecting flux and fouling during reverse osmosis of seawater, Desalination 151 (2002) 239–245.
[31] H. Chu, F. Zhao, X. Tan, L. Yang, X. Zhou, J. Zhao, Y. Zhang, The impact of temperature on membrane fouling in algae harvesting, Algal Res. 16 (2016) 458–464.
[32] M.F.A. Goosen, S.S. Sablani, S.S. Al-Maskari, R.H. Al-Belushi, M. Wilf, Effect of feed temperature on permeate flux and mass transfer coefficient in spiral-wound reverse osmosis systems, Desalination 144 (2002) 367–372.
[33] M. Kasi, H. Simsek, S. Ahlschlager, K. Ritterman, J. Hausauer, J. Hoff, E. Khan, Impact of operations and cleaning on membrane fouling at a wastewater reclamation facility, J. Environ. Manag. 193 (2017) 326–333.
[34] A. Abhishek Shrivastava, S. Rosenberg, M. Peery, Energy efficiency breakdown of reverse osmosis and its implications on future innovation roadmap for desalination, Desalination 368 (2015) 181–192.
[35] B.A. Qureshi, S.M. Zubair, Energy-exergy analysis of seawater reverse osmosis plants, Desalination 385 (2016) 138–147.
[36] A.M. Blanco-Marigorta, A. Lozano-Medina, J.D. Marcos, The exergetic efficiency as a performance evaluation tool in reverse osmosis desalination plants in operation, Desalination 413 (2017) 19–28.
[37] E. Dimitriou, P. Boutikos, E.S. Mohamed, S. Koziel, G. Papadakis, Theoretical performance prediction of a reverse osmosis desalination membrane element under variable operating conditions, Desalination 419 (2017) 70–78.
[38] G.E.B. Archer, A. Saltelli, I.M. Sobol, Sensitivity measures, anova like techniques and the use of bootstrap, J. Stat. Comput. Simul. 58 (1997) 99–120.
[39] G.E. Giap, N. Kosuke, Sensitivity analysis using Sobol 'variance-based method on the Haverkamp constitutive functions implemented in Richards' water flow equation, Malays. J. Soil Sci. 18 (2014) 19–33.
[40] J.R. Gat, A. Shemesh, E. Tziperman, A. Hecht, D. Georgopoulos, O. Basturk, The stable isotope composition of waters of the eastern Mediterranean Sea, J. Geophys. Res. 101 (C3) (1996) 6441–6451.
[41] K.C. Emeis, U. Struck, H.M. Schulz, R. Rosenberg, S. Bernasconi, H. Erlenkeuser, T. Sakamoto, F. Martinez-Ruiz, Temperature and salinity variations of Mediterranean Sea surface waters over the last 16,000 years from records of planktonic stable oxygen isotopes and alkenone unsaturation ratios, Palaeogeogr. Palaeoclimatol. Palaeoecol. 158 (2000) 259–280.
[42] M.M. Alhazmy, Economic and thermal feasibility of multi stage flash desalination plant with brine-feed mixing and cooling, Energy 76 (2014) 1029–1035.
[43] H.T. El-Dessouky, H.M. Ettouney, Fundamentals of Salt Water Desalination, 1st edition, Elsevier, 2002.